HHS Public Access

Author manuscript

Biol Psychiatry Cogn Neurosci Neuroimaging. Author manuscript; available in PMC 2017 January 01.

Published in final edited form as:

Biol Psychiatry Cogn Neurosci Neuroimaging. 2016 January 1; 1(1): 39–48. doi:10.1016/j.bpsc.2015.10.001.

Striatal magnetic resonance spectroscopy abnormalities in young adult SAPAP3 knockout mice

Dionyssios Mintzopoulos, Ph.D., **Timothy E. Gillis, Ph.D.**, **Holly R. Robertson, Ph.D.**, **Triana Dalia**, **Guoping Feng, Ph.D.**, **Scott L. Rauch, M.D.**, and **Marc J. Kaufman, Ph.D.**

Abstract

Background—Obsessive compulsive disorder (OCD) is a debilitating condition with lifetime prevalence of 1–3%. OCD typically arises in youth but delays in diagnosis impede optimal treatment and developmental studies of the disorder. Research using genetically modified rodents may provide models of etiology that enable earlier detection and intervention. The SAPAP3 knockout (KO) transgenic mouse was developed as an animal model of OCD and related disorders (OCRD). KO mice exhibit compulsive self-grooming behavior analogous to behaviors found in people with OCRD. Striatal hyperactivity has been reported in these mice and in humans with OCD.

Methods—Striatal and medial frontal cortex 9.4 Tesla proton spectra were acquired from young adult SAPAP3 KO and wild-type control mice to determine whether KO mice have metabolic and neurochemical abnormalities.

Results—Young adult KO mice had lower striatal lactate (P=0.006) and glutathione (P=0.039) levels. Among all mice, striatal lactate and glutathione levels were associated (R=0.73, P=0.007). We found no group differences in medial frontal cortex metabolites. At the age range studied, only 1 of 8 KO mice had skin lesions indicative of severe compulsive grooming.

Conclusion—Young adult SAPAP3 KO mice have striatal but not medial frontal cortex MRS abnormalities that may reflect striatal hypermetabolism accompanied by oxidative stress. These abnormalities typically preceded the onset of severe compulsive grooming. Our findings are consistent with striatal hypermetabolism in OCD. Together, these results suggest that striatal MRS

Address Correspondence to: Marc J. Kaufman, Ph.D., McLean Imaging Center MS 204, McLean Hospital, 115 Mill St., Belmont, MA 02478 USA, kaufman@mclean.harvard.edu.

Disclosures

Co-authors Mintzopoulos, Gillis, Robertson, Dalia, and Kaufman report no biomedical financial interests or potential conflicts of interest. Dr. Feng receives research funding from NIMH, Simons Foundation, Nancy Lurie Marks Family Foundation, Massachusetts Life Science Center, Brain Research Foundation and royalties from Washington University and Duke University. He is a scientific founder and a member of Board of Directors of Rugen Therapeutic Inc. He receives honoraria for advisory board service from the John Merck Fund. He also receives consulting fees from Taisho Pharmaceutical Co., Ltd. Dr. Rauch has received research funding from NIMH, US Army and royalties from APPI and Oxford University Press. He further receives honoraria for advisory board service from the Harvard Football Players Health Study. He is employed by, and receives salary from McLean Hospital/Partners Healthcare. Dr. Rauch also holds leadership roles with the SOBP, APA, NNDC and ADAA.

measures of lactate or glutathione might be useful biomarkers for early detection of risk for developing compulsive behavior disorders.

Keywords

Magnetic resonance spectroscopy; Obsessive compulsive disorder; Oxidative stress; SAPAP3 protein; Striatal dysfunction; Translational model

Introduction

Obsessive compulsive disorder (OCD) is among the most disabling health conditions (1) and has a lifetime prevalence estimated at 1–3%. OCD involves persistent, intrusive, thoughts and impulses (obsessions) and repetitive, intentional behaviors (compulsions). Although medication and behavioral therapy, available since the 1980s, are useful, they control symptoms with only limited success, the course of OCD remains chronic in most cases, and cure is rare. OCD typically arises in youth but often is diagnosed many years after initial symptoms appear (2). Delays in diagnosis impede optimal treatment as well as the study of pathogenesis of the disorder. Moreover, as reflected in the DSM-5, OCD is conceptualized among a spectrum of potentially related repetitive behavior disorders, Obsessive Compulsive and Related Disorders (OCRD), including Trichotillomania (hair-pulling), Hoarding Disorder, and Body Dysmorphic Disorder (3). A better understanding of etiology for these disorders could lead to early diagnosis and enable early intervention. Research using genetically modified rodents may ultimately provide models of etiology, pathophysiology, and pathogenesis that enable earlier detection and intervention for such disorders. For example, studies in the Slitrk5 knockout (KO) mouse model of OCRD, which exhibit compulsive grooming behavior and increased anxiety, revealed orbitofrontal hyperactivity (4). Other studies in the deer mouse, which is considered a naturalistic model of compulsive behavior disorders because these mice exhibit spontaneous stereotypy, revealed frontal cortex oxidative stress (5).

Another animal model of OCRD, the SAPAP3 KO mouse (6), exhibits cortico-striatal-thalamic-cortical (CSTC) circuit dysfunction thought to be a core feature of OCD (7). Biochemical, electrophysiological, and optogenetic studies reveal CSTC circuit defects in mutant mice (6, 8, 9). SAPAP3 protein, also known as DLGAP3, is a key scaffold protein for the assembly of the glutamatergic cortico-striatal synapses and the SAPAP3/DLGAP3 gene has been associated with OCRD and is considered a candidate gene for the DSM-5 Tic disorder, Tourette syndrome (TS) (10–13). Deletion of the SAPAP3 gene in mice results in severe compulsive grooming behavior that leads to facial hair removal and skin lesions, as well as anxiety-like behavior (6). Compulsive grooming and anxiety in KO mice are alleviated rapidly, within 6 days, by treatment with fluoxetine (6), a selective serotonin reuptake inhibitor (SSRI) and first line medication for OCD patients.

SAPAP3 KO mice exhibit substantially increased resting state striatal medium spiny neuron (MSN) firing rates (9). As MSNs comprise nearly 90% of all neurons within rodent striatum (14), their tonic hyperactivity in mutant mice could lead to a striatal hypermetabolic state similar to that detected with Positron Emission Tomography in people with OCD (15–18).

Moreover, increased activation of striatum in OCD as detected by functional imaging has been associated with OCD symptoms (e.g., 19) and relieved by successful treatment (20). Studies of OCRD and TS also report striatal structural (e.g., 21–22) and functional (e.g., 23–24) abnormalities, further supporting the hypothesis that the striatal node of the CSTC circuit is a critical element of compulsive behavior disorders.

Striatal fast-spiking parvalbumin-positive (PV+) GABA inhibitory potently inhibit striatal MSN firing and modulate action selection behavior (25–26), and their reduction in SAPAP3 KO mice (9) could contribute to striatal MSN hyperactivity and abnormal behaviors. Restoration of SAPAP3 KO mouse PV+ interneuron activity via lateral orbitofrontal cortico-striatal optogenetic stimulation normalizes overgrooming behavior (9), suggesting that PV+ interneurons play a key role in mediating compulsive behaviors in these mice. Interestingly, caudate nucleus and putamen PV+ interneuron densities also are reduced in people with TS (27–28) and PV gene expression is reduced in prefrontal cortex in humans with OCRD (29). Accordingly, it appears that PV+ interneuron abnormalities may be a common feature of compulsive behavior disorders in rodents and humans. SAPAP3 KO mice appear to model some key aspects of OCRD in humans and thus may be useful for helping to elucidate the etiology, pathophysiology, and pathogenesis of these disorders.

In this study, we used 9.4 Tesla proton magnetic resonance spectroscopy (MRS), a noninvasive imaging method well-suited for longitudinal and translational investigations, to determine whether SAPAP3 KO mice have striatal and medial frontal cortex neurochemical abnormalities. As noted above, existing data suggest that glutamatergic and GABAergic neurotransmission abnormalities, as well as metabolic stress, may exist in KO mice. Further, preclinical studies in the deer mouse model of compulsive behavior disorders identified cortical glutathione depletion, indicative of oxidative stress (5). That finding is consistent with a clinical trial reporting efficacy of N-acetylcysteine (NAC), a glutamate modulator that also acts as a glutathione precursor (30), in humans with OCD (31). Two clinical trials also reported NAC efficacy in nail biting disorder, which also is an OCRD (32, 33). Accordingly, we hypothesized that young adult SAPAP3 KO mice would exhibit abnormalities in striatal MRS metabolites related to neurotransmission, energy metabolism, and oxidative stress.

Methods and Materials

Mice

SAPAP3 KO mice were generated from a C57 mouse strain at the Massachusetts Institute of Technology (MIT) in Cambridge, MA as previously described (6). Adult female mice were transported from MIT to McLean Hospital by courier for scanning. Animals were housed in groups of four (two wild-type controls (WT) and two SAPAP3 KO) in polycarbonate cages and maintained on a 12:12 h light/dark cycle in a temperature- (22 °C) and humidity-controlled vivarium. Mice were acclimated for 36–48 hours prior to imaging, which occurred when mice were 3.5–5 months old (Figure 1). This age range was selected to determine whether MRS abnormalities could be detected before the onset of the severe compulsive grooming phenotype accompanied by skin lesions, which are 100% penetrant in SAPAP3 KO mice by about 6 months of age (6). Separate age-matched cohorts of WT and

KO mice were scanned using identical procedures, except MRS data were acquired from left striatum or medial frontal cortex (Figure 1). Food and water were available *ad libitum*. All animal procedures were approved by the MIT and McLean Hospital Institutional Animal Care and Use Committees and were conducted in accordance with the National Institutes of Health Guide for the Care and Use of Laboratory Animals (8th Edition).

Magnetic resonance imaging and spectroscopy procedures

MRI images and MRS spectra were acquired in vivo from isoflurane-anesthetized (1.5–2%) mice using a 9.4 Tesla horizontal-bore scanner equipped with a 60 mm ID, 100 G/cm, imaging gradient (Varian Inc., Direct Drive) and a custom-made volume coil. Physiological parameters, including rectal temperature, respiration rate, and heart rate/ECG, were monitored and maintained throughout all scans (Small Animal Instruments, Inc.). For MRS, three multi-slice images were acquired orthogonally along sagittal, axial, and coronal planes to guide placement of left striatal and medial frontal cortex voxels. MRS abnormalities in people with OCRD have been identified in left and right striatal structures (34). Because there is no evidence for a lateralized striatal abnormality in SAPAP3 KO mice and because of practical limitations of scanning time with anesthesia, we unilaterally studied left striatum. A 2D fast spin echo coronal MRI acquisition (TR = 2.1 s, TE = 60 ms, in-plane acquisition matrix 128 × 128, 0.17 mm × 0.17 mm × 0.5 mm imaging voxel size) was acquired, on which a striatal (2 × 2 × 2 mm = 8μL) or a medial frontal cortex (2.5 × 2 × 3 mm = 15μL) voxel was superimposed and visualized for optimized placement (Figure 2, insets).

MRS spectra were acquired using an ultra-short echo-time STEAM (35) sequence with TR=4 s and TE=3 ms, 4096 complex points, 5000 Hz acquisition bandwidth, 1 ms 90° excitation pulse. Voxel shimming was carried out using FASTMAP (36), which typically resulted in unsuppressed water line widths of 10–13 Hz. Then water spectra were acquired for preprocessing corrections and subsequent normalization. A water unsuppressed reference scan was acquired averaging the same sequence over a single phase cycle (four averages) with the water suppression amplitude set to zero, thus recording all effects of gradients. Water spectra were used for subsequent eddy-current correction and phasing of water-suppressed spectra (37). Then, free induction decays (FIDs) were acquired using a VAPOR water suppression scheme (38) with a 30 ms sinc pulse (200 Hz water suppression bandwidth), in groups of 128 averages (512 averages total, 34 min total acquisition time).

MRS data processing

MRS spectra were visually inspected and apodized with a 4 Hz exponential filter. Apodization was applied to filter high-frequency noise from the spectra while sharpening spectral features (Figure 2). This procedure was evaluated previously and resulted in good improvement in spectral quality without affecting data (39). The Klose correction, implemented in custom-written Matlab code (Mathworks, Inc, vR2012a), was used to correct the phase and any residual eddy currents using the phase of the unsuppressed water peak (37). FID blocks were added together using the NAA peak at 2 ppm to synchronize elimination of any residual frequency drift. Subsequently, spectra were automatically fitted with the LCModel (40) using a simulated basis set created with GAVA (41) and water-

scaling using the unsuppressed water peaks. Metabolites with Cramér-Rao Lower Bound values exceeding 30% were considered unreliable and were excluded from analyses. Areas of the unsuppressed water peaks were estimated after the data were phased and baseline corrected, with all steps carried out in MestreNova (MNOVA 9.0, Mestrelab.com). LCModel outputs (metabolite concentrations as reported in absolute institutional units by LCmodel) were transformed into ratios with a water denominator by dividing with the water integrals and scaling by an arbitrary multiplicative factor of 1000 for easier readability. Total glutathione was estimated using the glutamate and glycine moieties of glutathione via a standard weighted-sum formula in error analysis (42, 43). All steps were visually inspected against inadvertent errors.

Statistical Analysis

Two-sample two-tailed t tests were conducted using Stata software (v12, StataCorp, College Station, TX). The Grubb's outlier test (44) was applied to determine whether MRS measures were outliers.

Results

In each brain region, unsuppressed water peaks were statistically equivalent in WT and SAPAP3 KO mice (Table 1). Accordingly, unsuppressed water was used as a denominator to normalize metabolite levels within each voxel. In striatum, we found lower water-normalized lactate and glutathione (GSH) levels in KO versus WT mice (lactate/water: $p = 0.006$; GSH/water: $p = 0.039$, Table 1). None of the GSH or lactate values was identified as a statistical outlier. We did not detect group differences in any other striatal metabolite. In KO mice, we did not detect an association between age and either striatal lactate or GSH levels. However, when all mice were considered as a single group, we found a highly significant association between water-normalized striatal lactate and GSH levels ($R = 0.73$, $p = 0.007$, Figure 3). In medial frontal cortex, we did not detect group differences in any MRS metabolite, although in KO mice, there was a trend for higher total choline levels ($p < 0.08$, Table 1).

Only one of the 8 mutant mice in this study had developed skin lesions around the eyes, indicative of onset of severe compulsive self-grooming behavior. This mouse was one of the oldest mice in the study, just over 4.5 months of age at the time of the striatal MRS scan (Figure 1).

Discussion

Young adult SAPAP3 KO mice had lower striatal lactate and GSH levels than WT control type mice and among all mice undergoing striatal MRS, the levels of these two metabolites were strongly correlated. Together, these findings suggest that mutant mice experience a combination of striatal metabolic and oxidative stress. Within the age range studied (3.5 to 5.1 months old), we found no associations between age and either lactate or GSH levels in SAPAP3 KO mice, suggesting that MRS abnormalities may become apparent at younger ages. In addition, only one of the 8 mutant mice in this study exhibited fur patterns indicative of skin lesions. Since severe compulsive self-grooming behavior with fur

abnormality and skin lesions ultimately is 100% penetrant in SAPAP3 KO mice by about 6 months of age (6), our findings suggest that striatal lactate and GSH abnormalities generally precede the establishment of severe compulsive self-grooming behavior.

Medium spiny neurons are the predominant neuronal subtype within rodent striatum (14) and their tonic hyperactivity in SAPAP3 KO mice, which at rest exhibit 50% greater firing frequencies than WT mice (9), could be metabolically demanding and could trigger increased use of lactate to support the hypermetabolic state. In addition, mitochondrial oxidative stress resulting from metabolic stress can promote an adaptive switch to glycolysis to generate adenosine triphosphate (45), which could increase lactate catabolism. Either of these phenomena could lead, over time, to lower steady state striatal lactate levels. Lactate declines have been observed in healthy human visual cortex during prolonged visual stimulation (46), as well as in multiple cortical regions in bipolar disorder patients in the euthymic state, an effect attributed to increased metabolism/mitochondrial stress associated with mood normalization (47).

The striatal GSH reduction we detected in SAPAP3 KO mice may be indicative of oxidative stress. Because PV and GSH both play important roles in buffering oxidative stress, including stress induced by mitochondrial hydrogen peroxide (H_2O_2), one of the main reactive oxygen species (ROS) generated during mitochondrial oxidative metabolism (48), depletion of either antioxidant could result in depletion of both. PV+ interneurons produce especially high levels of H_2O_2 and other ROS and thus may be particularly vulnerable to oxidative stress (49). Accordingly, the GSH depletion we detected in SAPAP3 KO mice could be related or even contribute to the lower levels of striatal PV+ interneurons reported in these mice (9). Cerebral oxidative stress also can be engendered by anxiety, which is elevated in SAPAP3 KO mice (6). For example, in rodents, increased anxiety has been linked to higher levels of brain and blood ROS (50). Other anxiety-provoking conditions including restraint stress increase ROS levels (51–53). Further, chronic psychosocial stress has been reported to deplete hippocampal PV+ neurons in tree shrews (54). Thus, striatal hypermetabolism and anxiety in SAPAP3 KO mice could both enhance oxidative stress and reduce PV+ interneuron densities. Although fluoxetine's rapid normalization of compulsive behavior and anxiety in SAPAP3 KO mice (6) may be related to serotonin uptake inhibition, its efficacy could be mediated in part by fluoxetine's ability to buffer mitochondrial oxidative stress (55). Other serotonin uptake inhibitors and tricyclic antidepressants with efficacy for treating OCRD exhibit antioxidant properties (55), and their antioxidant effects could in part mediate clinical response.

Since striatal PV+ GABA interneuron expression is reduced in SAPAP3 KO mice by nearly 20% (9) and since PV+ neurons contain very high levels of GABA (56), we might have expected to detect lower GABA levels in KO mice. However, PV+ interneurons normally make up less than 1% of the total number of striatal GABA neurons (57); thus, a striatal GABA abnormality limited to PV+ interneurons could be difficult to detect with MRS. Further, PV expression can be dissociated from GABA neuron expression, for example, in mouse cortex, in which repeated ketamine treatments reduced PV+ interneuron counts by more than 30% without altering GABA interneuron numbers (58). Similarly, PV+ interneuron reductions have been reported without concomitant changes in GABA levels in

maternal Ube3a KO mice (59). That being said, the KO mouse with skin lesions indicative of severe compulsive grooming had the lowest striatal GABA level of all mice in the study, 5.97, more than 1 standard deviation below the KO group mean (Table 1). That mouse also had striatal glutamate and NAA levels (49.23 and 40.23, respectively) nearly 1 standard deviation below KO group means (Table 1). Future studies in older mice will be necessary to confirm whether striatal MRS metabolite abnormalities worsen after the onset of severe compulsive grooming.

Our finding of no group difference in striatal glutamate is inconsistent with an MRS report of abnormally elevated striatal glutamate in pediatric OCD, which declined after paroxetine treatment (60). This apparent discrepancy could be related to species, methodological, genetics, or other differences. However, our null finding in SAPAP3 KO mice is consistent with a recent report in medication-free adults with OCD using optimized striatal glutamate detection methods (61). As noted above, striatal glutamate abnormalities may become apparent in older SAPAP3 KO mice, especially after the onset of severe compulsive grooming.

Our medial frontal cortex null finding was somewhat unexpected since this brain area is part of the CSTC circuitry implicated in OCRD (7) and since other mouse models of compulsive behavior disorders, including Slitrk5 KO and deer mice, both exhibit frontal cortex abnormalities (4, 5). However, our finding is consistent with a recent human study in people with OCD conducted by our group reporting no glutamate or other MRS metabolite abnormalities in rostral anterior cingulate cortex (62). Collectively, the results in mouse models could suggest that functional deficits in frontal cortex and/or striatum may be sufficient to alter CSTC circuitry and enable compulsive behaviors. This possibility is supported by findings showing that several days of brief repetitive optogenetic stimulation of medial orbital frontal cortex in wild-type mice engenders cortical and striatal hyperactivation along with persisting compulsive self-grooming behavior, which can be alleviated by fluoxetine (63).

The present MRS findings further illustrate the utility of the SAPAP3 KO mouse as a translational model for OCRD. Striatal hypermetabolism in SAPAP3 KO mice, manifest as lower lactate levels, appears to parallel striatal glucose hypermetabolism reported in humans with OCRD or TS (15–18, 64). Similarly, the striatal oxidative stress we found in SAPAP3 KO mice, manifest as a GSH reduction, appears to parallel reports of peripheral oxidative stress both in children and adults with OCRD or TS (65–71). One of these reports (66) noted a strong association between OCD clinical severity (measured with the Yale Brown Obsessive Compulsive Scale) and a serum marker of lipid peroxidation, suggesting that peripheral oxidative stress markers in people with OCRD could be associated with or related to central abnormalities. Polymorphisms of the neuronal glutamate transporter (EAAC1) gene, which mediates cysteine uptake necessary for neuronal GSH production (72), have been associated with OCD (for review, see 73), further suggesting a link between abnormal GSH levels and OCD.

Although cerebral oxidative stress has not been reported in OCRD, a randomized controlled trial of NAC reduced OCD symptoms (31), and as noted above, NAC efficacy has been

reported in people nail biting disorder (32, 22), further supporting the possibility that cerebral oxidative stress contributes to these disorders. NAC prevents oxidative stress-induced impairments in PV+ neuron development in preclinical models of schizophrenia (74, 75) and could have similar effects in OCRD. Dopamine, which is rapidly auto-oxidized to generate ROS (76), is a potential source of striatal oxidative stress in OCRD. In this regard, patients with OCRD or TS have been reported to exhibit higher striatal synaptic dopamine levels (77–82). Higher striatal dopamine transporter densities also have been reported in OCRD and TS patients (83–86), which could enhance striatal intracellular dopamine auto-oxidation, ROS formation, and oxidative stress (87).

The parallels between SAPAP3 KO mice and humans with OCRD also suggest that MRS measures of striatal lactate or GSH could be abnormal in humans with these disorders. While a number of striatal MRS studies in people with OCRD have been published (see 34 for review; and 61, 88–92), none reported on lactate or GSH levels. This is due in part to the fact that MRS scan sequences used previously in humans were not optimal for quantifying these metabolites in striatum. The present findings suggest that MRS measurements of striatal lactate and GSH levels using optimized acquisition methods could be informative in people with or at risk for developing OCRD.

Limitations

This study has a number of limitations including its small sample sizes and its cross-sectional design. The striatum was selected as a main focus for our initial study because it is a target for the SAPAP3 mutation and it is known to be abnormal based on histochemical and electrophysiological measurements in SAPAP3 KO mice (6, 8, 9). The present findings suggest that at least with respect to MRS measures, the striatum is more severely affected than medial frontal cortex in young adult SAPAP3 KO mice. It will be important in future studies to determine whether lactate, GSH, and other MRS metabolite abnormalities exist in mutant mice in the thalamus, another CSTC circuit region, as well as in other brain areas. Our findings also suggest that additional MRS studies are necessary during early brain development and in later adulthood, to determine when MRS abnormalities emerge and whether they worsen once severe compulsive grooming behavior has been established. We expect that lactate depletions may correspond with grooming or anxiety severity, as OCD clinical severity is positively associated with striatal glucose metabolic rate (93, 94) and OCD symptoms are associated with striatal activation (e.g., 19). We also expect that lactate and GSH may normalize with fluoxetine treatment, as striatal glucose metabolism normalizes with effective OCD treatment (20, 95, 96). Another limitation of this study is our use of isoflurane anesthesia, which can acutely increase brain lactate levels, possibly by impairing mitochondrial oxidative metabolism (97). However, since all mice in this study were administered isoflurane at the same concentration and for the same duration, it seems unlikely that the group difference we detected in striatal lactate levels can be attributed solely to isoflurane anesthesia. While we are not aware of any MRS studies reporting effects of isoflurane on GSH levels, isoflurane anesthesia did not alter liver, kidney, lung, or blood GSH levels in mice (98). To overcome the potential confound of isoflurane anesthesia, we plan future studies with anesthetic regimens that differentially affect lactate and other MRS metabolite levels (97). Also, in future studies, we will analyze grooming behavior to

determine whether MRS abnormalities detected presently are related to or predictive of grooming behavior severity and the development of skin lesions. Another limitation of this study is the relatively large voxel sizes we used, which covered either the entire left striatum or multiple frontal cortex subregions; thus, we cannot discriminate between medial and lateral or dorsal versus ventral striatal subdivisions, which play different roles in behavioral control (99), or between medial orbital and prelimbic/infralimbic frontal cortical areas, which may be differentially affected in SAPAP3 KO mice.

Conclusions

Our findings suggest that SAPAP3 KO mice exhibit striatal hypermetabolism and oxidative stress. The data support the need for future longitudinal studies in KO mice to assess the time courses of lactate and GSH changes in striatum and other brain regions, to determine whether associations exist between lactate or GSH levels and striatal PV+ interneuron densities, and to determine whether existing and experimental interventions normalize MRS and striatal PV+ interneuron abnormalities. Our findings also suggest that MRS studies of striatal lactate and GSH levels in humans with OCRD could be informative and potentially lead to the development of new methods for early diagnosis and treatment.

Acknowledgments

This research was supported by a generous grant from James and Patricia Poitras, by NIH grant S10 RR019356, and by the Counter-Drug Technology Assessment Center (CTAC), an office within the Office of National Drug Control Policy (ONDCP), via Contract Number DBK39-03-C-0075 awarded by the Army Contracting Agency. The content of the information does not necessarily reflect the position or the policy of the Government and no official endorsement should be inferred. We thank Dr. Brian Brennan for reviewing and commenting on the manuscript.

References

(Note: these will be renumbered in the final version).

1. Kessler RC, Aguilar-Gaxiola S, Alonso J, Chatterji S, Lee S, Ormel J, et al. The global burden of mental disorders: an update from the WHO World Mental Health (WMH) surveys. Epidemiol Psichiatr Soc. 2009; 18:23–33. [PubMed: 19378696]
2. Stengler K, Olbrich S, Heider D, Dietrich S, Riedel-Heller S, Jahn I. Mental health treatment seeking among patients with OCD: impact of age of onset. Soc Psychiatry Psychiatr Epidemiol. 2013; 48:813–819. [PubMed: 22763495]
3. American Psychiatric Association. Diagnostic and Statistical Manual of Mental Disorders: DSM-5. Washington, D.C: American Psychiatric Press; 2013.
4. Shmelkov SV, Hormigo A, Jing D, Proenca CC, Bath KG, Milde T, et al. Slitrk5 deficiency impairs corticostriatal circuitry and leads to obsessive-compulsive-like behaviors in mice. Nat Med. 2010; 16:598–602. [PubMed: 20418887]
5. Güldenpfennig M, de Wolmarans W, du Preez JL, Stein DJ, Harvey BH. Cortico-striatal oxidative status, dopamine turnover and relation with stereotypy in the deer mouse. Physiol Behav. 2011; 103:404–11. [PubMed: 21397620]
6. Welch JM, Lu J, Rodriguiz RM, Trotta NC, Peca J, Ding JD, et al. Cortico-striatal synaptic defects and OCD-like behaviours in Sapap3-mutant mice. Nature. 2007; 448:894–900. [PubMed: 17713528]
7. Graybiel AM, Rauch SL. Toward a neurobiology of obsessive-compulsive disorder. Neuron. 2000; 28:343–347. [PubMed: 11144344]
8. Wan Y, Feng G, Calakos N. Sapap3 deletion causes mGluR5-dependent silencing of AMPAR synapses. J Neurosci. 2011; 31:16685–16691. [PubMed: 22090495]

9. Burguière E, Monteiro P, Feng G, Graybiel AM. Optogenetic stimulation of lateral orbitofronto-striatal pathway suppresses compulsive behaviors. Science. 2013; 340:1243–1246. [PubMed: 23744950]
10. Bienvenu OJ, Wang Y, Shugart YY, Welch JM, Grados MA, Fyer AJ, et al. Sapap3 and pathological grooming in humans: Results from the OCD collaborative genetics study. Am J Med Genet B Neuropsychiatr Genet. 2009; 150B:710–720. [PubMed: 19051237]
11. Züchner S, Wendland JR, Ashley-Koch AE, Collins AL, Tran-Viet KN, Quinn K, et al. Multiple rare SAPAP3 missense variants in trichotillomania and OCD. Mol Psychiatry. 2009; 14:6–9. [PubMed: 19096451]
12. Boardman L, van der Merwe L, Lochner C, Kinnear CJ, Seedat S, Stein DJ, et al. Investigating SAPAP3 variants in the etiology of obsessive-compulsive disorder and trichotillomania in the South African white population. Compr Psychiatry. 2011; 52:181–187. [PubMed: 21295225]
13. Crane J, Fagerness J, Osiecki L, Gunnell B, Stewart SE, Pauls DL, et al. Family-based genetic association study of DLGAP3 in Tourette Syndrome. Am J Med Genet B Neuropsychiatr Genet. 2011; 156B:108–114. [PubMed: 21184590]
14. Graveland GA, DiFiglia M. The frequency and distribution of medium-sized neurons with indented nuclei in the primate and rodent neostriatum. Brain Res. 1985; 327:307–311. [PubMed: 3986508]
15. Baxter LR Jr, Phelps ME, Mazziotta JC, Guze BH, Schwartz JM, Selin CE. Local cerebral glucose metabolic rates in obsessive-compulsive disorder. A comparison with rates in unipolar depression and in normal controls. Arch Gen Psychiatry. 1987; 44:211–218. [PubMed: 3493749]
16. Baxter LR Jr, Schwartz JM, Mazziotta JC, Phelps ME, Pahl JJ, Guze BH, Fairbanks L. Cerebral glucose metabolic rates in nondepressed patients with obsessive-compulsive disorder. Am J Psychiatry. 1988; 145:1560–1563. [PubMed: 3264118]
17. Perani D, Colombo C, Bressi S, Bonfanti A, Grassi F, Scarone S, et al. [18F]FDG PET study in obsessive-compulsive disorder. A clinical/metabolic correlation study after treatment. Br J Psychiatry. 1995; 166:244–250. [PubMed: 7728370]
18. Zuo C, Ma Y, Sun B, Peng S, Zhang H, Eidelberg D, et al. Metabolic imaging of bilateral anterior capsulotomy in refractory obsessive compulsive disorder: an FDG PET study. J Cereb Blood Flow Metab. 2013; 33:880–887. [PubMed: 23443174]
19. Rauch SL, Jenike MA, Alpert NM, Baer L, Breiter HC, Savage CR, et al. Regional cerebral blood flow measured during symptom provocation in obsessive-compulsive disorder using ^{15}O-labeled CO_2 and positron emission tomography. Arch Gen Psychiatry. 1994; 51:62–70. [PubMed: 8279930]
20. Schwartz JM, Stoessel PW, Baxter LR Jr, Martin KM, Phelps ME. Systematic changes in cerebral glucose metabolic rate after successful behavior modification treatment of obsessive-compulsive disorder. Arch Gen Psychiatry. 1996; 53:109–113. [PubMed: 8629886]
21. Plessen KJ, Bansal R, Peterson BS. Imaging evidence for anatomical disturbances and neuroplastic compensation in persons with Tourette syndrome. J Psychosom Res. 2009; 67:559–573. [PubMed: 19913660]
22. Rauch SL, Phillips KA, Segal E, Makris N, Shin LM, Whalen PJ, et al. A preliminary morphometric magnetic resonance imaging study of regional brain volumes in body dysmorphic disorder. Psychiatry Res. 2003; 122:13–19. [PubMed: 12589879]
23. Feusner JD, Moody T, Hembacher E, Townsend J, McKinley M, Moller H, et al. Abnormalities of visual processing and frontostriatal systems in body dysmorphic disorder. Arch Gen Psychiatry. 2010; 67:197–205. [PubMed: 20124119]
24. Mazzone L, Yu S, Blair C, Gunter BC, Wang Z, Marsh R, et al. An FMRI study of frontostriatal circuits during the inhibition of eye blinking in persons with Tourette syndrome. Am J Psychiatry. 2010; 167:341–349. [PubMed: 20080981]
25. Koós T, Tepper JM. Inhibitory control of neostriatal projection neurons by GABAergic interneurons. Nat Neurosci. 1999; 2:467–472. [PubMed: 10321252]
26. Gage GJ, Stoetzner CR, Wiltschko AB, Berke JD. Selective activation of striatal fast-spiking interneurons during choice execution. Neuron. 2010; 67:466–79. [PubMed: 20696383]

27. Kalanithi PS, Zheng W, Kataoka Y, DiFiglia M, Grantz H, Saper CB, et al. Altered parvalbumin-positive neuron distribution in basal ganglia of individuals with Tourette syndrome. Proc Natl Acad Sci U S A. 2005; 102:13307–13312. [PubMed: 16131542]
28. Kataoka Y, Kalanithi PS, Grantz H, Schwartz ML, Saper C, Leckman JF, et al. Decreased number of parvalbumin and cholinergic interneurons in the striatum of individuals with Tourette syndrome. J Comp Neurol. 2010; 518:277–291. [PubMed: 19941350]
29. Jaffe AE, Deep-Soboslay A, Tao R, Hauptman DT, Kaye WH, Arango V, et al. Genetic neuropathology of obsessive psychiatric syndromes. Transl Psychiatry. 2014; 4:e432. [PubMed: 25180571]
30. Samuni Y, Goldstein S, Dean OM, Berk M. The chemistry and biological activities of N-acetylcysteine. Biochim Biophys Acta. 2013; 1830:4117–4129. [PubMed: 23618697]
31. Afshar H, Roohafza H, Mohammad-Beigi H, Haghighi M, Jahangard L, Shokouh P, et al. N-acetylcysteine add-on treatment in refractory obsessive-compulsive disorder: a randomized, double-blind, placebo-controlled trial. J Clin Psychopharmacol. 2012; 32:797–803. [PubMed: 23131885]
32. Berk M, Jeavons S, Dean OM, Dodd S, Moss K, Gama CS, et al. Nail-biting stuff? The effect of N-acetyl cysteine on nail-biting. CNS Spectr. 2009; 14:357–360. [PubMed: 19773711]
33. Ghanizadeh A, Derakhshan N, Berk M. N-acetylcysteine versus placebo for treating nail biting, a double blind randomized placebo controlled clinical trial. Antiinflamm Antiallergy Agents Med Chem. 2013; 12:223–228. [PubMed: 23651231]
34. Brennan BP, Rauch SL, Jensen JE, Pope HG Jr. A critical review of magnetic resonance spectroscopy studies of obsessive-compulsive disorder. Biol Psychiatry. 2013; 73:24–31. [PubMed: 22831979]
35. Frahm J, Merboldt KD, Hänicke W. Localized proton spectroscopy using stimulated echoes. J Magn Reson. 1987; 72:502–508.
36. Gruetter R. Automatic, localized in vivo adjustment of all first- and second-order shim coils. Magn Reson Med. 1993; 29:804–811. [PubMed: 8350724]
37. Klose U. In vivo proton spectroscopy in presence of eddy currents. Magn Reson Med. 1990; 14:26–30. [PubMed: 2161984]
38. Tkác I, Starcuk Z, Choi IY, Gruetter R. In vivo 1H NMR spectroscopy of rat brain at 1 ms echo time. Magn Reson Med. 1999; 41:649–656. [PubMed: 10332839]
39. Puhl MD, Mintzopoulos D, Jensen JE, Gillis TE, Konopaske GT, Kaufman MJ, et al. In vivo magnetic resonance studies reveal neuroanatomical and neurochemical abnormalities in the serine racemase knockout mouse model of schizophrenia. Neurobiol Dis. 2014; 73C:269–274. [PubMed: 25461193]
40. Provencher SW. Estimation of metabolite concentrations from localized in vivo proton NMR spectra. Magn Reson Med. 1993; 30:672–679. [PubMed: 8139448]
41. Soher BJ, Young K, Bernstein A, Aygula Z, Maudsley AA. GAVA: spectral simulation for in vivo MRS applications. J Magn Reson. 2007; 185:291–299. [PubMed: 17257868]
42. Bevington, PR.; Robinson, DK. Data Reduction and Error Analysis for the Physical Sciences. New York: Mc Graw Hill Higher Education; 2002.
43. Provencher, SW. [Accessed February 2, 2014] LCModel & LCMgui User's Manual. http://s-provencher.com/pub/LCModel/manual/manual.pdf
44. Grubbs F. Procedures for Detecting Outlying Observations in Samples. Technometrics. 1969; 11:1–21.
45. Wu SB, Wu YT, Wu TP, Wei YH. Role of AMPK-mediated adaptive responses in human cells with mitochondrial dysfunction to oxidative stress. Biochim Biophys Acta. 2014; 1840:1331–1344. [PubMed: 24513455]
46. Mangia S, Tkác I, Logothetis NK, Gruetter R, Van de Moortele PF, Uğurbil K. Dynamics of lactate concentration and blood oxygen level-dependent effect in the human visual cortex during repeated identical stimuli. J Neurosci Res. 2007; 85:3340–3346. [PubMed: 17526022]
47. Brady RO Jr, Cooper A, Jensen JE, Tandon N, Cohen B, Renshaw P, et al. A longitudinal pilot proton MRS investigation of the manic and euthymic states of bipolar disorder. Transl Psychiatry. 2012; 2:e160. [PubMed: 22968227]

48. Permyakov SE, Kazakov AS, Avkhacheva NV, Permyakov EA. Parvalbumin as a metal-dependent antioxidant. Cell Calcium. 2014; 55:261–268. [PubMed: 24685310]
49. Kann O, Papageorgiou IE, Draguhn A. Highly energized inhibitory interneurons are a central element for information processing in cortical networks. J Cereb Blood Flow Metab. 2014; 34:1270–1282. [PubMed: 24896567]
50. Rammal H, Bouayed J, Younos C, Soulimani R. Evidence that oxidative stress is linked to anxiety-related behaviour in mice. Brain Behav Immun. 2008; 22:1156–1159. [PubMed: 18620042]
51. Madrigal JL, Olivenza R, Moro MA, Lizasoain I, Lorenzo P, Rodrigo J, et al. Glutathione depletion, lipid peroxidation and mitochondrial dysfunction are induced by chronic stress in rat brain. Neuropsychopharmacology. 2001; 24:420–429. [PubMed: 11182537]
52. Chakraborti A, Gulati K, Banerjee BD, Ray A. Possible involvement of free radicals in the differential neurobehavioral responses to stress in male and female rats. Behav Brain Res. 2007; 179:321–325. [PubMed: 17368574]
53. Sahin E, Gümüşlü S. Immobilization stress in rat tissues: alterations in protein oxidation, lipid peroxidation and antioxidant defense system. Comp Biochem Physiol C Toxicol Pharmacol. 2007; 144:342–347. [PubMed: 17157074]
54. Czeh B, Simon M, van der Hart MG, Schmelting B, Hesselink MB, Fuchs E. Chronic stress decreases the number of parvalbumin-immunoreactive interneurons in the hippocampus: prevention by treatment with a substance P receptor (NK1) antagonist. Neuropsychopharmacology. 2005; 30:67–79. [PubMed: 15470372]
55. Steiner JP, Bachani M, Wolfson-Stofko B, Lee MH, Wang T, Li G, et al. Interaction of paroxetine with mitochondrial proteins mediates neuroprotection. Neurotherapeutics. 2015; 12:200–216. [PubMed: 25404050]
56. Chesselet MF, Plotkin JL, Wu N, Levine MS. Development of striatal fast-spiking GABAergic interneurons. Prog Brain Res. 2007; 160:261–272. [PubMed: 17499119]
57. Luk KC, Sadikot AF. GABA promotes survival but not proliferation of parvalbumin-immunoreactive interneurons in rodent neostriatum: an in vivo study with stereology. Neuroscience. 2001; 104:93–103. [PubMed: 11311534]
58. Powell SB, Sejnowski TJ, Behrens MM. Behavioral and neurochemical consequences of cortical oxidative stress on parvalbumin-interneuron maturation in rodent models of schizophrenia. Neuropharmacology. 2012; 62:1322–1331. [PubMed: 21315745]
59. Godavarthi SK, Sharma A, Jana NR. Reversal of reduced parvalbumin neurons in hippocampus and amygdala of Angelman syndrome model mice by chronic treatment of fluoxetine. J Neurochem. 2014; 130:444–454. [PubMed: 24678582]
60. Rosenberg DR, MacMaster FP, Keshavan MS, Fitzgerald KD, Stewart CM, Moore GJ. Decrease in caudate glutamatergic concentrations in pediatric obsessive-compulsive disorder patients taking paroxetine. J Am Acad Child Adolesc Psychiatry. 2000; 39:1096–1103. [PubMed: 10986805]
61. Simpson HB, Kegeles LS, Hunter L, Mao X, Van Meter P, Xu X, et al. Assessment of glutamate in striatal subregions in obsessive-compulsive disorder with proton magnetic resonance spectroscopy. Psychiatry Res. 2015; 232:65–70. [PubMed: 25715904]
62. Brennan BP, Tkachenko O, Schwab ZJ, Juelich RJ, Ryan EM, Athey AJ, et al. An Examination of Rostral Anterior Cingulate Cortex Function and Neurochemistry in Obsessive-Compulsive Disorder. Neuropsychopharmacology. 2015; 40:1866–1876. [PubMed: 25662837]
63. Ahmari SE, Spellman T, Douglass NL, Kheirbek MA, Simpson HB, Deisseroth K, et al. Repeated cortico-striatal stimulation generates persistent OCD-like behavior. Science. 2013; 340(6137): 1234–1239. [PubMed: 23744948]
64. Braun AR, Randolph C, Stoetter B, Mohr E, Cox C, Vladar K, et al. The functional neuroanatomy of Tourette's syndrome: an FDG-PET Study. II: Relationships between regional cerebral metabolism and associated behavioral and cognitive features of the illness. Neuropsychopharmacology. 1995; 13:151–168. [PubMed: 8597526]
65. Behl A, Swami G, Sircar SS, Bhatia MS, Banerjee BD. Relationship of possible stress-related biochemical markers to oxidative/antioxidative status in obsessive-compulsive disorder. Neuropsychobiology. 2010; 61:210–214. [PubMed: 20389131]

66. Chakraborty S, Singh OP, Dasgupta A, Mandal N, Nath Das H. Correlation between lipid peroxidation-induced TBARS level and disease severity in obsessive-compulsive disorder. Prog Neuropsychopharmacol Biol Psychiatry. 2009; 33:363–366. [PubMed: 19272303]

67. Kandemir H, Abuhandan M, Aksoy N, Savik E, Kaya C. Oxidative imbalance in child and adolescent patients with obsessive compulsive disorder. J Psychiatr Res. 2013; 47:1831–1834. [PubMed: 24011862]

68. Kuloglu M, Atmaca M, Tezcan E, Gecici O, Tunckol H, Ustundag B. Antioxidant enzyme activities and malondialdehyde levels in patients with obsessive-compulsive disorder. Neuropsychobiology. 2002; 46:27–32. [PubMed: 12207144]

69. Landau YE, Steinberg T, Richmand B, Leckman JF, Apter A. Involvement of immunologic and biochemical mechanisms in the pathogenesis of Tourette's syndrome. J Neural Transm. 2012; 119:621–626. [PubMed: 22139323]

70. Orhan N, Kucukali CI, Cakir U, Seker N, Aydin M. Genetic variants in nuclear-encoded mitochondrial proteins are associated with oxidative stress in obsessive compulsive disorders. J Psychiatr Res. 2012; 46:212–218. [PubMed: 22070905]

71. Ozdemir E, Cetinkaya S, Ersan S, Kucukosman S, Ersan EE. Serum selenium and plasma malondialdehyde levels and antioxidant enzyme activities in patients with obsessive-compulsive disorder. Prog Neuropsychopharmacol Biol Psychiatry. 2009; 33:62–65. [PubMed: 18957313]

72. Aoyama K, Suh SW, Hamby AM, Liu J, Chan WY, Chen Y, Swanson RA. Neuronal glutathione deficiency and age-dependent neurodegeneration in the EAAC1 deficient mouse. Nat Neurosci. 2006; 9:119–126. [PubMed: 16311588]

73. Monteiro P, Feng G. Learning from animal models of Obsessive-Compulsive Disorder. Biol Psychiatry. in press.

74. Cabungcal JH, Steullet P, Kraftsik R, Cuenod M, Do KQ. Early-life insults impair parvalbumin interneurons via oxidative stress: reversal by N-acetylcysteine. Biol Psychiatry. 2013; 73:574–582. [PubMed: 23140664]

75. Cabungcal JH, Counotte DS, Lewis EM, Tejeda HA, Piantadosi P, Pollock C, et al. Juvenile antioxidant treatment prevents adult deficits in a developmental model of schizophrenia. Neuron. 2014; 83:1073–1084. [PubMed: 25132466]

76. Kulagina NV, Michael AC. Monitoring hydrogen peroxide in the extracellular space of the brain with amperometric microsensors. Anal Chem. 2003; 75:4875–4881. [PubMed: 14674466]

77. Denys D, van der Wee N, Janssen J, De Geus F, Westenberg HG. Low level of dopaminergic D2 receptor binding in obsessive-compulsive disorder. Biol Psychiatry. 2004; 55:1041–1045. [PubMed: 15121489]

78. Denys D, de Vries F, Cath D, Figee M, Vulink N, Veltman DJ, et al. Dopaminergic activity in Tourette syndrome and obsessive-compulsive disorder. Eur Neuropsychopharmacol. 2013; 23:1423–1431. [PubMed: 23876376]

79. Moresco RM, Pietra L, Henin M, Panzacchi A, Locatelli M, Bonaldi L, et al. Fluvoxamine treatment and D2 receptors: a pet study on OCD drug-naïve patients. Neuropsychopharmacology. 2007; 32:197–205. [PubMed: 17019408]

80. Olver JS, O'Keefe G, Jones GR, Burrows GD, Tochon-Danguy HJ, Ackermann U, et al. Dopamine D1 receptor binding in the striatum of patients with obsessive-compulsive disorder. J Affect Disord. 2009; 114:321–326. [PubMed: 18706700]

81. Perani D, Garibotto V, Gorini A, Moresco RM, Henin M, Panzacchi A, et al. In vivo PET study of 5HT(2A) serotonin and D(2) dopamine dysfunction in drug-naive obsessive-compulsive disorder. Neuroimage. 2008; 42:306–314. [PubMed: 18511303]

82. Singer HS, Szymanski S, Giuliano J, Yokoi F, Dogan AS, Brasic JR, et al. Elevated intrasynaptic dopamine release in Tourette's syndrome measured by PET. Am J Psychiatry. 2002; 159:1329–1336. [PubMed: 12153825]

83. Kim CH, Koo MS, Cheon KA, Ryu YH, Lee JD, Lee HS. Dopamine transporter density of basal ganglia assessed with [123I]IPT SPET in obsessive-compulsive disorder. Eur J Nucl Med Mol Imaging. 2003; 30:1637–1643. [PubMed: 14513291]

84. Kim CH, Cheon KA, Koo MS, Ryu YH, Lee JD, Chang JW, et al. Dopamine transporter density in the basal ganglia in obsessive-compulsive disorder, measured with [123I]IPT SPECT before and

after treatment with serotonin reuptake inhibitors. Neuropsychobiology. 2007; 55:156–162. [PubMed: 17657168]

85. Liu H, Dong F, Meng Z, Zhang B, Tan J, Wang Y. Evaluation of Tourette's syndrome by (99m)Tc-TRODAT-1 SPECT/CT imaging. Ann Nucl Med. 2010; 24:515–521. [PubMed: 20544324]
86. Serra-Mestres J, Ring HA, Costa DC, Gacinovic S, Walker Z, Lees AJ, et al. Dopamine transporter binding in Gilles de la Tourette syndrome: a [123I]FP-CIT/SPECT study. Acta Psychiatr Scand. 2004; 109:140–146. [PubMed: 14725596]
87. Masoud ST, Vecchio LM, Bergeron Y, Hossain MM, Nguyen LT, Bermejo MK, et al. Increased expression of the dopamine transporter leads to loss of dopamine neurons, oxidative stress and l-DOPA reversible motor deficits. Neurobiol Dis. 2015; 74:66–75. [PubMed: 25447236]
88. DeVito TJ, Drost DJ, Pavlosky W, Neufeld RW, Rajakumar N, McKinlay BD, et al. Brain magnetic resonance spectroscopy in Tourette's disorder. J Am Acad Child Adolesc Psychiatry. 2005; 44:1301–1308. [PubMed: 16292123]
89. Gnanavel S, Sharan P, Khandelwal S, Sharma U, Jagannathan NR. Neurochemicals measured by (1)H-MR spectroscopy: putative vulnerability biomarkers for obsessive compulsive disorder. MAGMA. 2014; 27:407–417. [PubMed: 24338164]
90. Tükel R, Aydın K, Ertekin E, Özyıldırım SŞ, Taravari V. Proton magnetic resonance spectroscopy in obsessive-compulsive disorder: evidence for reduced neuronal integrity in the anterior cingulate. Psychiatry Res. 2014; 224:275–280. [PubMed: 25241042]
91. Tükel R, Aydın K, Ertekin E, Özyıldırım SŞ, Barburoğlu M. 1H-magnetic resonance spectroscopy in obsessive-compulsive disorder: effects of 12 weeks of sertraline treatment on brain metabolites. Eur Arch Psychiatry Clin Neurosci. 2015; 265:219–226. [PubMed: 25256264]
92. Whiteside SP, Abramowitz JS, Port JD. Decreased caudate N-acetyl-l-aspartic acid in pediatric obsessive-compulsive disorder and the effects of behavior therapy. Psychiatry Res. 2012; 202:53–59. [PubMed: 22704757]
93. Hansen ES, Hasselbalch S, Law I, Bolwig TG. The caudate nucleus in obsessive-compulsive disorder. Reduced metabolism following treatment with paroxetine: a PET study. Int J Neuropsychopharmacol. 2002; 5:1–10. [PubMed: 12057027]
94. Kwon JS, Kim JJ, Lee DW, Lee JS, Lee DS, Kim MS, et al. Neural correlates of clinical symptoms and cognitive dysfunctions in obsessive-compulsive disorder. Psychiatry Res. 2003; 122:37–47. [PubMed: 12589881]
95. Baxter LR Jr, Schwartz JM, Bergman KS, Szuba MP, Guze BH, Mazziotta JC, et al. Caudate glucose metabolic rate changes with both drug and behavior therapy for obsessive-compulsive disorder. Arch Gen Psychiatry. 1992; 49:681–689. [PubMed: 1514872]
96. Kang DH, Kwon JS, Kim JJ, Youn T, Park HJ, Kim MS, et al. Brain glucose metabolic changes associated with neuropsychological improvements after 4 months of treatment in patients with obsessive-compulsive disorder. Acta Psychiatr Scand. 2003; 107:291–297. [PubMed: 12662252]
97. Boretius S, Tammer R, Michaelis T, Brockmöller J, Frahm J. Halogenated volatile anesthetics alter brain metabolism as revealed by proton magnetic resonance spectroscopy of mice in vivo. Neuroimage. 2013; 69:244–255. [PubMed: 23266699]
98. Zumbiel MA, Fiserova-Bergerova V, Malinin TI, Holaday DA. Glutathione depletion following inhalation anesthesia. Anesthesiology. 1978; 49:102–108. [PubMed: 28682]
99. Baldan Ramsey LC, Xu M, Wood N, Pittenger C. Lesions of the dorsomedial striatum disrupt prepulse inhibition. Neuroscience. 2011; 180:222–228. [PubMed: 21315809]

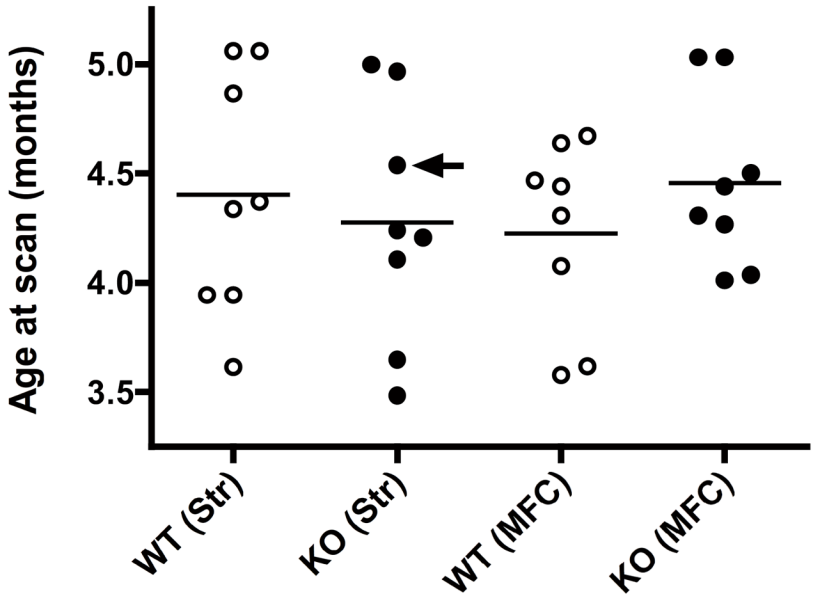

Figure 1.

Age distributions of wild type control (WT) and SAPAP3 knockout (KO) mice in this study stratified by genotype and MRS brain area: left striatum (Str) or medial frontal cortex (MFC). Mean ages are shown for each group as horizontal lines. The arrow identifies the mouse with skin lesions, indicative of the severe compulsive grooming phenotype.

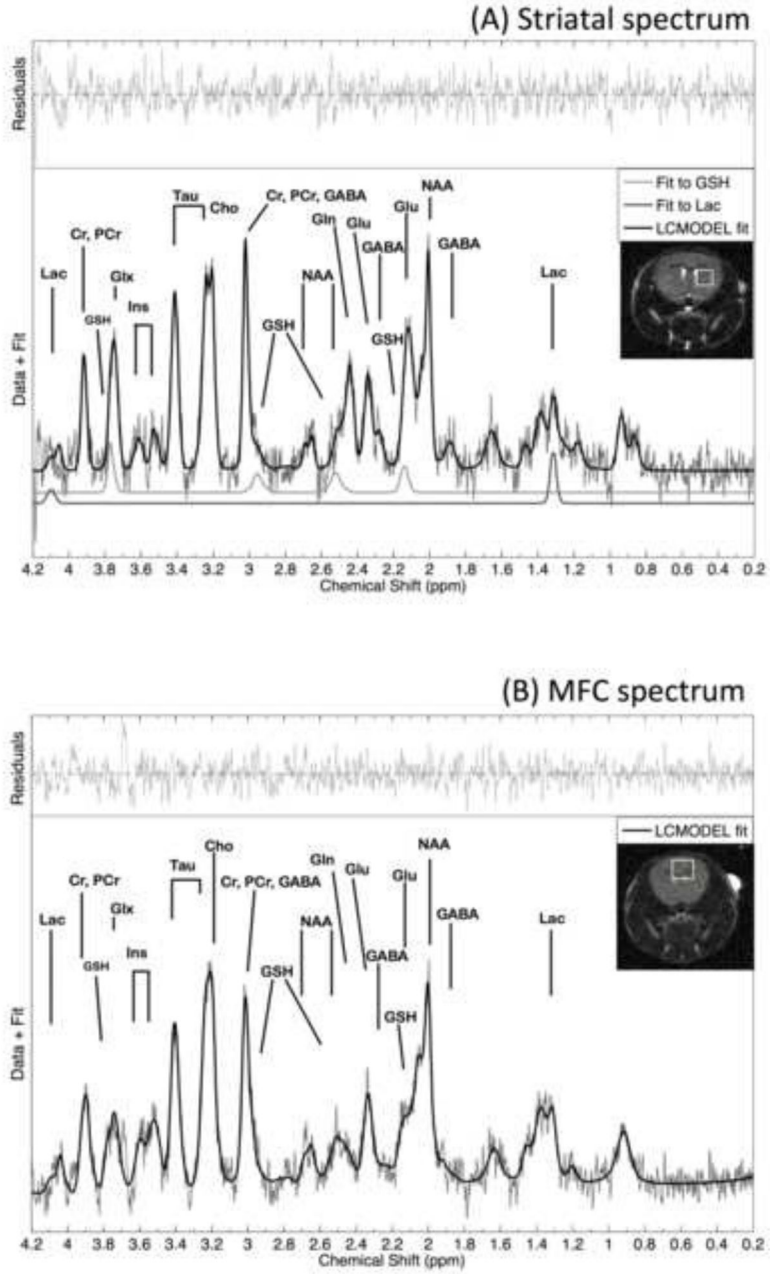

Figure 2.

Representative left striatal (Panel a) and medial frontal cortex (Panel b) spectra and LCmodel fits and residual fits from wild-type control mice. LCmodel fits for striatal lactate and glutathione are shown separately (Panel a). Insets illustrate positions of a left striatal MRS voxel (Panel a) and a medial frontal cortex voxel (Panel b) superimposed onto coronal brain slices. The following metabolites are identified: Choline: Cho; Creatine: Cr, GABA; Glutamate: Glu; Glutamine: Gln; Glutamate/glutamine: Glx; Glutathione: GSH; myo-inositol (Ins); Lactate: Lac; N-acetylaspartate: NAA; Phosphocreatine: PCr; Taurine: Tau.

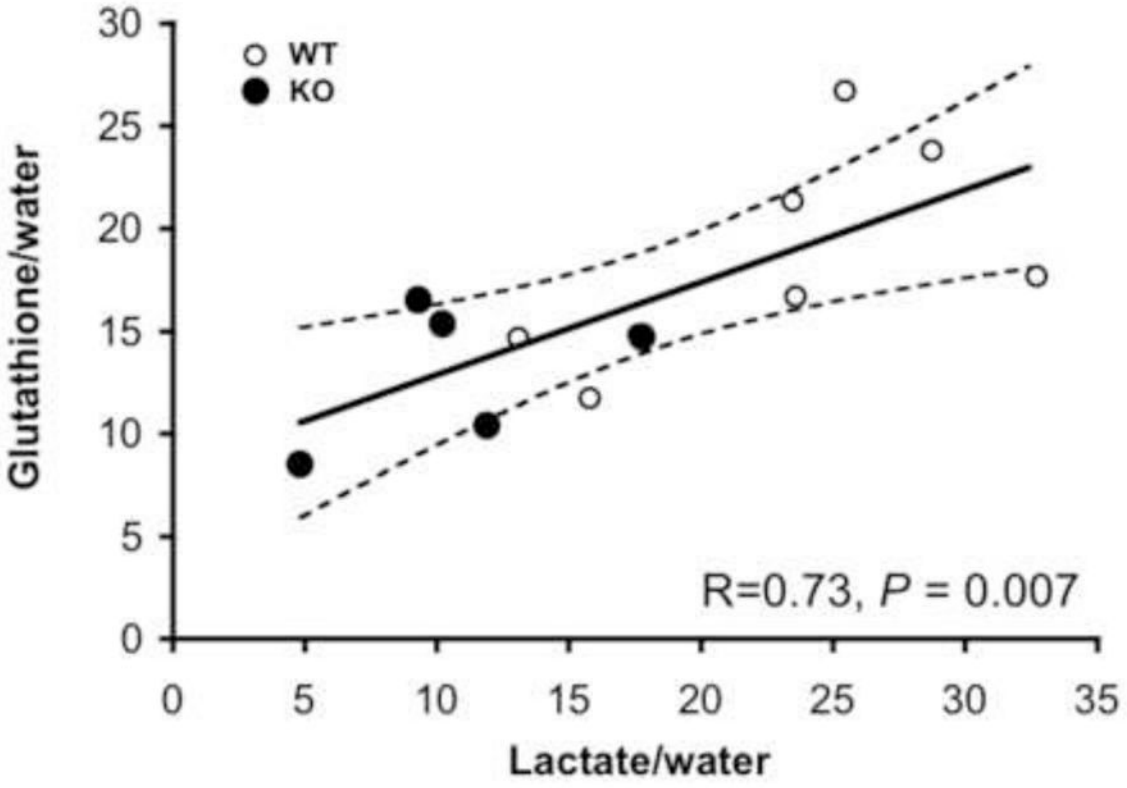

Figure 3.

Correlation plot showing the relationship between striatal water normalized lactate and glutathione levels (including only measurements with Cramér-Rao Lower Bound (CRLB) values ≤ 30%). Wild type mice (WT, N=7, 1 mouse had a lactate CRLB <30%) are shown as open circles and SAPAP3 knockout mice (KO, N=5, 3 mice had lactate CRLBs <30%) are shown as filled circles. Also shown is the 95% confidence interval.

Table 1

Striatal and medial frontal cortex proton MRS measures in SAPAP3 knockout (KO) and wild-type control (WT) mice

MRS Measure	WT[†]	KO[†]	P-values[§]	(t-statistic, df)
Striatum				
GABA/H_2O	23.28 ± 4.15 (8)	19.80 ± 8.39 (8)	0.310	(1.052, 14)
Gln/H_2O	41.53 ± 29.06 (8)	31.08 ± 10.17 (8)	0.353	(0.960, 14)
Glu/H_2O	74.02 ± 14.34 (8)	67.51 ± 23.69 (8)	0.517	(0.665, 14)
Gly/H_2O	19.25 ± 9.72 (6)	18.48 ± 10.51 (5)	0.903	(0.125, 9)
GSH/H_2O	18.08 ± 5.46 (8)	13.00 ± 3.21 (8)	0.039 *	(2.273, 14)
Ins/H_2O	50.51 ± 14.15 (8)	53.36 ± 20.09 (8)	0.748	(−0.328, 14)
Lac/H_2O	23.26 ± 6.87 (7)	10.77 ± 4.64 (5)	0.006 **	(3.508, 10)
NAA/H_2O	63.60 ± 11.66 (8)	56.03 ± 17.86 (8)	0.332	(1.004, 14)
Tau/H_2O	130.21 ± 29.81 (8)	106.02 ± 45.22 (8)	0.227	(1.263, 14)
tCho/H_2O	16.97 ± 3.52 (8)	17.57 ± 7.03 (8)	0.832	(−0.216, 14)
tCr/H_2O	79.83 ± 14.93 (8)	75.99 ± 32.51 (8)	0.766	(0.304, 14)
H_2O	2056 ± 196 (8)	2121 ± 123 (8)	0.436	(−0.801, 14)
Medial Frontal Cortex				
GABA/H_2O	10.62 ± 6.08 (7)	12.28 ± 5.89 (8)	0.602	0.535, 13
Gln/H_2O	23.28 ± 15.34 (6)	29.88 ± 20.21 (7)	0.527	0.654, 11
Glu/H_2O	50.23 ± 17.23 (8)	64.39 ± 17.09 (8)	0.121	1.650, 14
Gly/H_2O	22.46 ± 19.53 (6)	19.88 ± 15.28 (5)	0.816	−0.240, 9
GSH/H_2O	13.14 ± 4.65 (8)	13.55 ± 9.43 (7)	0.916	0.108, 13
Ins/H_2O	25.30 ± 13.94 (8)	32.30 ± 13.55 (8)	0.308	1.058, 14
Lac/H_2O	12.13 ± 7.67 (6)	13.66 ± 5.24 (4)	0.740	0.344, 8
NAA/H_2O	40.36 ± 10.93 (8)	42.11 ± 11.20 (8)	0.756	0.316, 14
Tau/H_2O	61.64 ± 20.77 (8)	77.02 ± 32.04 (8)	0.274	1.139, 14
tCho/H_2O	8.45 ± 1.69 (8)	14.68 ± 9.00 (8)	0.075	1.923, 14
tCr/H_2O	49.24 ± 16.62 (8)	58.63 ± 19.71 (8)	0.320	1.030, 14
H_2O	2348 ± 303 (8)	2384 ± 261 (8)	0.801	0.257, 14

WT= wild type; KO = SAPAP3 knockout; df = degrees of freedom; Gln = glutamine; Glu = glutamate; Gly = glycine; GSH = glutathione; Ins = myo-inositol; Lac = lactate; NAA = N-acetylaspartate; Tau = Taurine; tCho = total choline; tCr = total creatine;

[†] Mean ± SD (N);

[§] 2-sided values,

* $P \leq 0.05$;

** $P \leq 0.01$.

Only measurements with Cramér-Rao Lower Bound (CRLB) values ≤ 30% are included. Measures with Ns < 8 and dfs < 14 indicate that some CRLB values exceeded 30%. Separate cohorts of WT and KO mice were used to acquire striatal or medial frontal cortex MRS scans.